

Long term monitoring of the Balladelaan bridge using smart Aggregates

C.N. Kortendijk¹, A. Hoekstra¹, F. Besseling¹, Y. Yang², H. Cheng²

¹Witteveen+Bos Consulting Engineers, Leeuwenbrug 8, 7411TJ Deventer, Netherlands

²Department of Engineering Structures, Faculty of Civil Engineering and GeoSciences, Delft University of Technology, Stevinweg 1, 2628CN Delft, Netherlands

email: coen.kortendijk@witteveenbos.com, Anke.Hoekstra@witteveenbos.com, Floris.Besseling@witteveenbos.com, Yuguang.Yang@tudelft.nl, H.Cheng-2@tudelft.nl

ABSTRACT: The Balladelaan Bridge is a key bridge in the city of Amersfoort. The city has asked us to investigate the construction quality and remaining lifespan of this 5 span statically indeterminate cast-in-place concrete plate bridge, which was built in 1946. For this a pioneering long-term Structural Health Monitoring (SHM) initiative has been implemented in the form of a Field lab employing Smart Aggregates (SA's) using Coda-Wave Interferometry (CWI), augmented with extensive temperature measurements, and a short-term measurement using Acoustic Emission (AE) sensors. This study represents an extensive application of Smart Aggregates for continuous monitoring of a bridge's structural health over an extended period. The study aims to address the suitability of SA's for long term monitoring and accounting for environmental influences such as temperature and humidity on the wave speed in the concrete. Preliminary findings demonstrate a significant influence of temperature on wave speed readings, underscoring the necessity of temperature compensation in SHM analysis. After accounting for these environmental influences, the study generates critical insights into the bridge's integrity and performance. The outcomes of this research will not only enhance the understanding of the Balladelaan Bridge's condition but also establish a benchmark for future SHM projects utilizing Smart Aggregates and CWI technology.

KEY WORDS: SHMII-13; Smart Aggregates; Structural Health Monitoring; Concrete; Bridges; Coda Wave Interferometry; Environmental Variability.

1 INTRODUCTION

Concrete slab bridges designed and built in the post WWII era, are relatively sensitive to shear failure. This raises concerns about the structural capacity of these bridges and the associated remaining service life.

Structural Health Monitoring (SHM) focuses in monitoring the variation of the structural performance a given structure with respect to selected dominant failure mechanisms. When it is properly designed, it enables asset managers to continuously track the evolution of the structural integrity of the bridge from the status without acquiring all the key information of the monitoring structure. This offers a significant advantage over traditional inspection methods, which often only involve periodic visual inspections.

For this a new monitoring solution using Smart Aggregates (SA's) has been installed on the Balladelaan bridge. SA sensors can be embedded or drilled into concrete to measure (changes in) stress and crack formation between sensor pairs. The installation of this field-lab has earlier been described by Cheng et al [1]. This paper describes the results of well over 1 year of continuous monitoring using SA's.

2 THE BALLADELAAN BRIDGE

The bridge in the Balladelaan in Amersfoort was built in 1946. It is a cast-in-place concrete bridge with 5 spans, which together form a statically indeterminate deck system. The bridge has one bus lane (1 lane), a cycle path and a pedestrian path. The bridge was chosen for its suitability:

- The multiple span configuration of the bridge allows to focus monitoring + data analysis on local response variations over time, as an indicator of damage.
- Because there is no normal car traffic on the bridge except a bus with known schedule, there is more certainty regarding the traffic load on the bridge. This makes calibration of models easier.
- Compared to new construction, lifespan extension with risk management by means of a monitoring system results in significantly lower costs and sustainability benefits.
- The bridge represents many equivalent concrete bridges in the Netherlands, so the knowledge gained here can be used more widely.



Figure 2-1 Side view of bridge (source: Google Streetview)



Figure 2-2 Top view of bridge (source: Google Maps)

3 SENSOR AND MONITORING SYSTEM

3.1 Smart aggregates

Smart aggregates (SA's) are embedded piezoelectric sensors that can measure (changes in) stress and formation of cracks in concrete between two sensors using interferometry of waves through the concrete. An example of such a system is shown in Figure 4-5. They were first introduced by Song et al[3], designed for long term monitoring of concrete structures. These sensors are embedded within concrete structures. This can be prior to casting for new constructions or afterwards through a drilled hole. They generate high-frequency elastic waves and receive them within the concrete. The received wave signals are logged and eventually analyzed. There is a relation between the wave propagation velocity and the stress on the concrete. Also, there is a relation between the shape of the waves and the existing cracks in the concrete. Smart aggregates should be able to detect this.

In a typical measurement, one SA functions as the transmitter while the remaining SA's in the cluster act as receivers. When a measurement begins, the measurement order is assigned remotely, and a high-voltage electric pulse is sent to the transmitter to initiate vibration. This electric pulse is converted into a mechanical wave that propagates through the concrete. Upon reaching the receivers, the wave signals are converted back into electrical signals, recorded as 1D time-series data, and stored locally at the data station.

3.2 Temperature sensors

Due to the static indeterminate structure of the bridge, it is expected that vertical temperature gradients due to sunlight will significantly influence the internal stress distribution in the bridge. The wave velocity in concrete is also temperature dependent. As these 2 factors will influence the signals measured by the smart aggregates, a significant amount of temperature sensors was installed to investigate this relationship, and in a later stage, compensate for this. Two systems were used in this particular setup:

- 1 PT1000 sensors. These are resistance-based sensors. They require a relatively short cable to a sensitive analog-to-digital converter.

- 2 DS18B20 sensors. These are digital sensors that support longer cables and can be read from a cheap microcontroller.

Both systems have a resolution of 0.01°C , and have been pre-calibrated in the lab to within 0.1°C accuracy. Part of this project was also to test the durability and reliability of both kinds of temperature sensors.

3.3 Acquisition system

The monitoring system comprises a data acquisition (DAQ) system for signals received by the SA's, an ARM embedded board for temperature measurements, and a 4G router with a SIM card for communication. The DAQ system, designed and patented by Delft University of Technology (TU Delft), is optimized for ultrasound-based monitoring of concrete structures.

The DAQ system includes a pulser, pre-amplifiers, and multiplexers. Thanks to the specialized circuit board design, the pulser can generate square pulses with a magnitude of up to 300 V without interfering with the received signals. For this project a single square-wave pulse with a duration $< 20 \mu\text{s}$ was used.

The data acquisition system supports a sampling rate of 3 MHz, enabling the recording of wave signals with frequencies up to 300 kHz without aliasing or loss of dynamics. This is well-suited for the requirements of ultrasound-based concrete monitoring applications. Each measurement lasts for 4 milliseconds from the moment the transmitter receives the electric pulse.

4 INSTALLATION AND DATA PROCESSING

4.1 Sensor locations

Sensors have been installed in both the center span, and an end-span of the bridge. Sensor positions are shown in Figure 4-1 to Figure 4-4. Distributed data acquisition systems are below the bridge with a main station including 4G router on shore.

The distance between the top and bottom SA's in each hole is fixed at 300 mm. During installation the top SA's are consistently positioned 175 mm beneath the top surface of the bridge slab, while the bottom SA's are set 475 mm below the top surface.

Sensors are grouped in three clusters of 3-4 holes, with 2 sensors per hole. The first cluster (hole A-D) is positioned to detect flexural crack development in midspan, which is crucial for detecting bridge flexural failure. The second (E-H) monitors stress changes or crack opening at intermediate supports. The third cluster (I-K) is placed to detect the initialization or progression of diagonal cracks in shear critical zones.

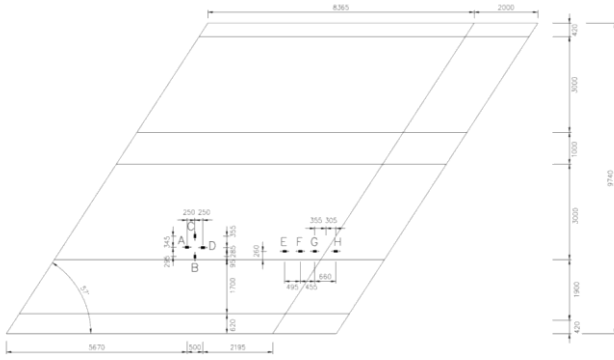


Figure 4-1 Top view SA-sensor locations center span

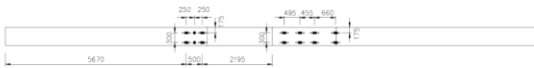


Figure 4-2 Side view SA-sensor locations center span

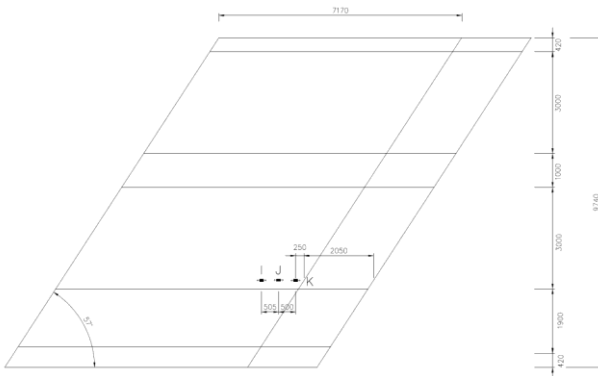


Figure 4-3 Top view SA-sensor locations end span



Figure 4-4 Side view SA-sensor locations end span

4.2 Installation process

Sensor preparation was conducted at TU Delft. SA's were affixed to copper wires using glue to ensure their alignment with the specified orientation and spacing, as illustrated in Figure 4-5. At select locations mentioned in Section 4, temperature sensors were also glued adjacent to the SA's on the copper wires to measure temperatures in close proximity to the sensor positions, as depicted in Figure 4-6.

The entire installation process followed these steps:

- Determining the rebar layout using a radar-based rebar detector.
- Identifying drilling locations based on the rebar layout.
- Drilling holes at the designated sensor locations
- Installing sensors into the drilled holes
- Filling the holes with high-strength mortar

- Installing the data acquisition systems and organizing cables
- Installing the main station on the bank.

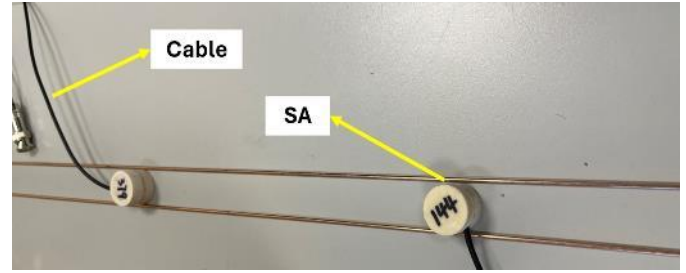


Figure 4-5 SA sensor at lab.

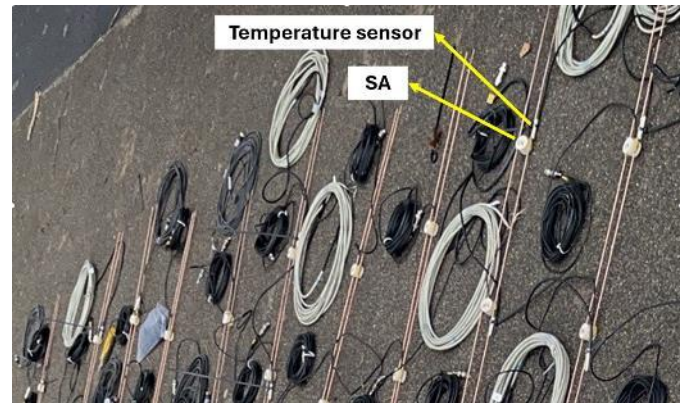


Figure 4-6 SA sensor in the field with added temperature sensors

4.3 Wave velocity processing

Changes in wave velocity are related to changes in stress-state of the concrete. The wave-velocity change can be determined by comparing the two signals in time. When the velocity changes are small (which we can assume here), we can assume a linear relation between travel time and wave velocity:

$$\frac{dv}{v} = -\frac{dt}{t}$$

This means that an increase in travel time is directly related to a decrease in velocity. We use the stretching technique to find this relative shift in time between two signals. With this technique the new signal is stretched in the time domain, relative to t_0 , which starts at the departure of the wave from the sending sensor, such that it fits the other signal (reference signal). Then this shift of the time axis between the signal and the reference signal is equal to the change in velocity.

With the stretching technique, we calculate correlation coefficients of windowed signals for the different delays.

$$CC(t_c, T, \epsilon) = \frac{\int_{t_c-T}^{t_c+T} u(t)u'(t(1-\epsilon))dt}{\sqrt{\int_{t_c-T}^{t_c+T} u(t)^2 dt} \sqrt{\int_{t_c-T}^{t_c+T} u'(t(1-\epsilon))^2 dt}}$$

t_c is the center of the time window, $2T$ is the duration of the time window and ϵ is the stretching factor. When there is an

uniform velocity change in the medium, one can assume that the correlation coefficient is maximum at the stretching factor that corresponds to the relative velocity change.

The stretching window can be chosen in different ways. It depends on the wave frequency: a window that is too short will not contain enough information. The window should also not be too large, because in that case you can no longer assume a constant time shift within the stretching window.

In this research, we limited ourselves to direct waveforms. These are the waves that travel in a straight line from one sensor to the other. One can assume that this is mainly the longitudinal / compression wave, because their wave speed is higher. Therefore, we selected a window containing only the first part of the signal, which contains approximately 2 cycles.

5 MEASUREMENT RESULTS

5.1 Initial measurements

Figure 5-1 presents a typical trace in the time domain from a measurement obtained from SA's. Similar patterns are observed for other sensor pairs but are not displayed here. The data shows a high signal to noise ratio, indicative of high quality.

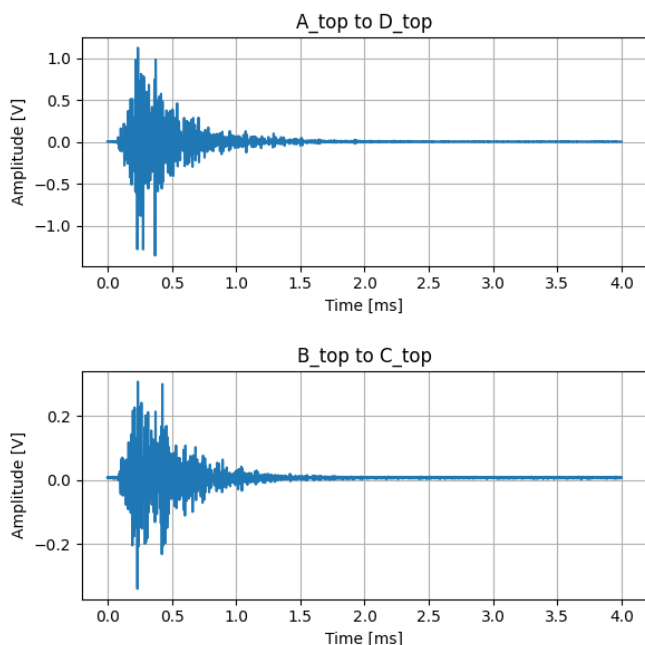


Figure 5-1 Trace of 2 sensor pairs

Figure 5-2 shows how on sunny days, a large temperature gradient between the top and bottom of the deck is observed, where the top of deck heats (and cools) faster than the bottom of the deck, which lags behind. All top temperatures show similar temperatures, with 1 sensor deviating. This sensor is on the end span, where the deck has some shade from neighboring trees.

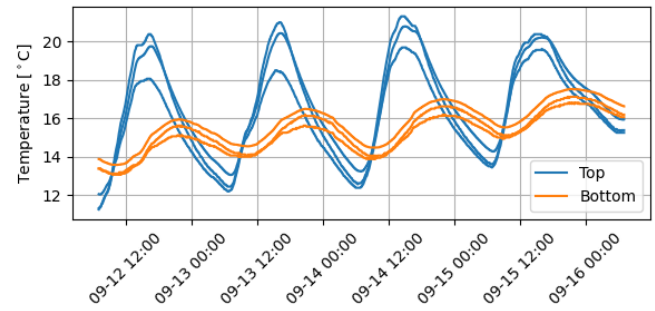


Figure 5-2 Temperatures in top and bottom of slab over 7 days

5.2 Wave velocity change

The resulting velocity change over time for a selected period is shown in the figure below. This period is chosen because it shows a large fluctuation in the measured temperature. The calculations are performed for two sensor pairs: A_top to D_top (Figure 5-3) and B_top to C_top (Figure 5-4). The velocity change is plotted together with the mean temperature measured in the bridge in this cluster by the temperature sensors.

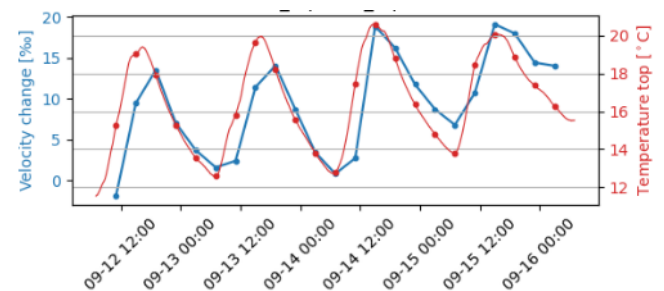


Figure 5-3 Temperature and velocity change A-D

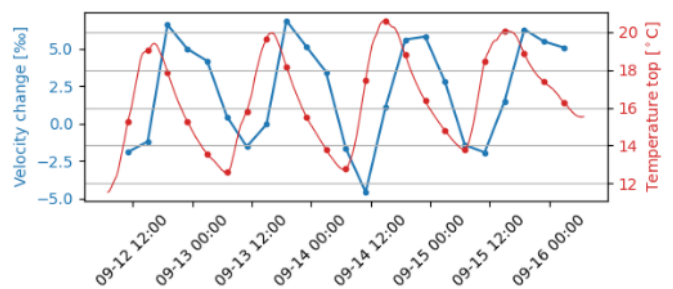


Figure 5-4 Temperature and velocity change B-C

The velocity changes in Figure 5-3 and Figure 5-4 are obtained by stretching a measurement signal until the maximum correlation between this signal and a predetermined previous signal is obtained. The resulting correlation coefficients as shown in Figure 5-5 are Figure 5-6 are an indicator of signal quality and may also indicate crack-opening. It can be seen that for the period shown the correlation coefficient is high (well over 0.8), indicating no significant crack change or deterioration of measurement equipment.

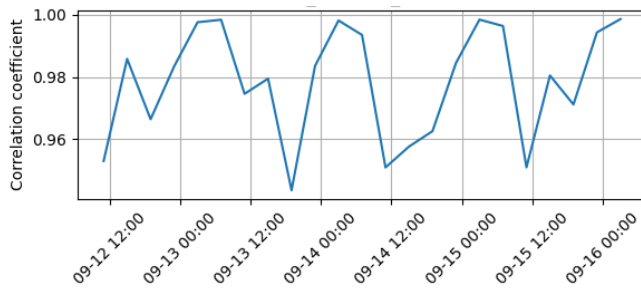


Figure 5-5 Correlation Coefficient A-D

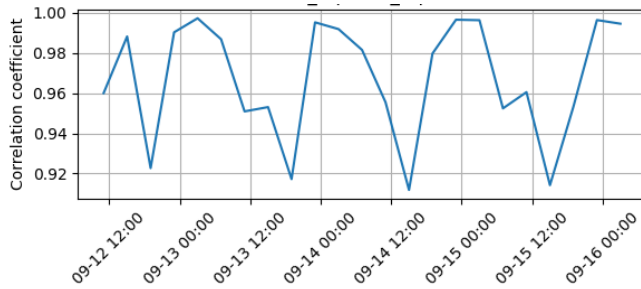


Figure 5-6 Correlation Coefficient B-C

Figure 5-3 implies a correlation between the velocity change of sensor pair A-D (and therefore the stress state of the material) and the temperature. This correlation is also seen in the scatter from Figure 5-5. It shows that with a higher temperature, there is an increase in the velocity.

This relation can also be observed in sensor pair B-C, but with an approximately 4-hour delay. After shifting the signal by four hours, a strong correlation is found, as shown in Figure 5-8.

The relation between temperature and velocity change and the accompanying time shift is not easily understood, as the velocity change is not only directly related to average concrete temperature. Due to the 5-span static-indeterminate system, the temperature gradients also induce stress which induces a velocity change. This will be different in the different directions that the sensor pairs have (A-D and B-C). Moreover, there is an overall temperature gradient within the bridge that fluctuates over time. The delay might be explained by the combination of different temperatures in the bridge. Further work will be to further analyze the temperature-induced changes in wave velocity.

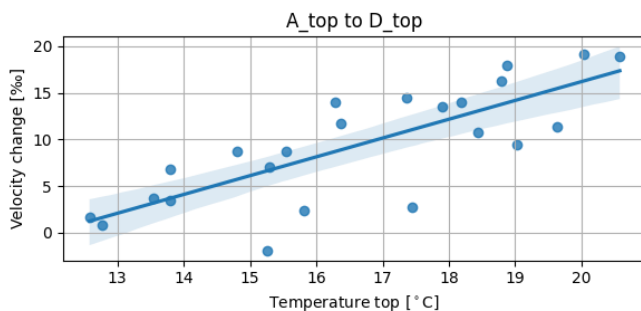


Figure 5-7 Temperature vs Velocity change A-D

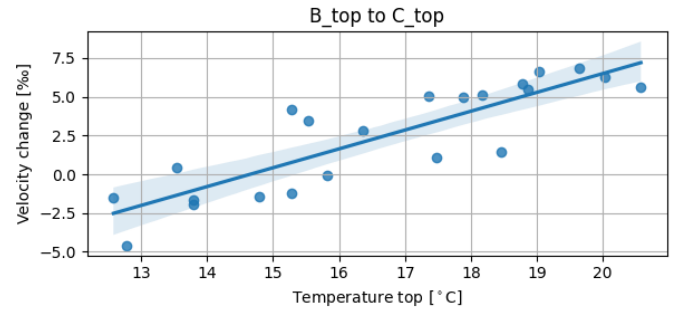


Figure 5-8 Temperature vs velocity change B-C after 4hr shift

5.3 Long term stability

The temperature sensors perform as expected. During well over one year of measurements, the concrete temperature has varied between -2.62°C and $+42.20^{\circ}\text{C}$, see Figure 5-9.

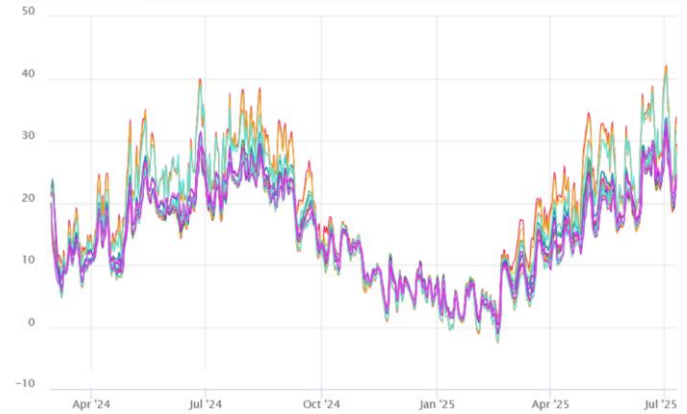


Figure 5-9 One year of temperature measurements

The digital DS18B20 sensors were unavailable for a short period of time due to a broken microcontroller, but this was easily fixed. In general, both types of sensors seem suitable for long term monitoring.

The SA-aggregates also perform well. After approximately 17 months of measurements each SA has sent and received approximately $500 \text{ days} \times 6 \text{ daily runs} \times 7 \text{ receiving SA's} \times 10 \text{ stacks} = 210000$ pulses. The sensors have been exposed to both freezing (-2.62°C) and high ($+42.20^{\circ}\text{C}$) temperatures, without failure. Proving the system is viable and stable for long-term measurements. Due to the nature of the system, no calibration of the built-in sensors is needed (or possible), while other sensor types may significantly degrade over time impacting repeatability.

As mentioned in 4.3 the change in wave velocity is calculated by finding the time stretching factor that results in maximum correlation coefficient between the current measurement and a specific previous measurement. The specific previous measurement may (in general) be chosen in two ways:

1. A(n average of a set of) reference measurement(s) just after installation is taken as the reference signal for all future measurements.

2. Each measurement is compared against its direct predecessor (in our case 4 hours earlier), or an average of a few direct predecessors.

After one year of measurements these two methods may be compared. Method 1 is shown in Figure 5-10. Here specific drops can be seen in early January for sensor pair A-D, and early March for pair B-C. In the first quarter of 2025 the wear-layer on the deck was replaced in multiple stages, which may have directly or indirectly caused this drop. The lower correlation coefficients may also negatively affect the accuracy of the time stretching.

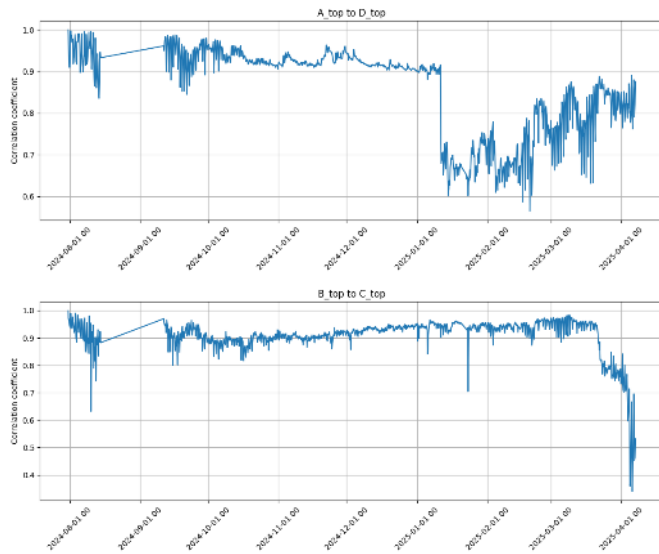


Figure 5-10 Correlation coefficient relative to first measurement

To obtain the optimal time stretching high correlation coefficients are preferred. This may be achieved by method 2, comparing each signal to its direct predecessor. In our case 4 hours earlier, as shown in Figure 5-11. Here high coefficients are obtained for most of the year. But during days with large temperature changes and accompanying temperature gradients (March-October as shown in Figure 5-9) the correlation coefficients also show variation. This variation is larger than it was in previous periods with similar temperature gradients, such as August 2024. A possible explanation might be that the replacement of the wear layer has induced (micro-)cracking in the high-strength mortar that was used to fill the drilled holes of the SA's.

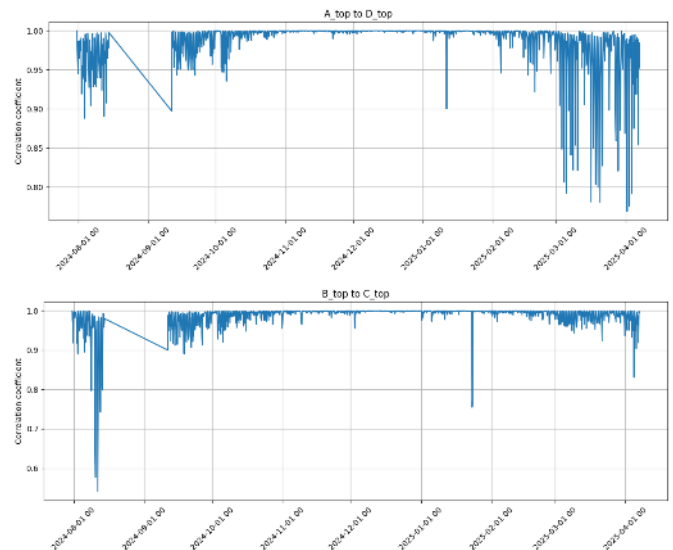


Figure 5-11 Correlation coefficient to 4hrs earlier

Both methods have their own advantages and disadvantages. Method 2 shows consistently high correlation coefficients, resulting in accurate stretch factors. But information about slow progressive changes over time are lost. Method 1 gives information relative to date of installation, but if the system is changed, correlation coefficients drop, and the stretch factors may be less accurate.

A solution may be found by combining both methods. Use method 1 until a significant drop in correlation coefficient is visible, indicating a change in the system which might be indicative of structural damage. Mark this point in time, and then apply all future processing relative to just after this event.

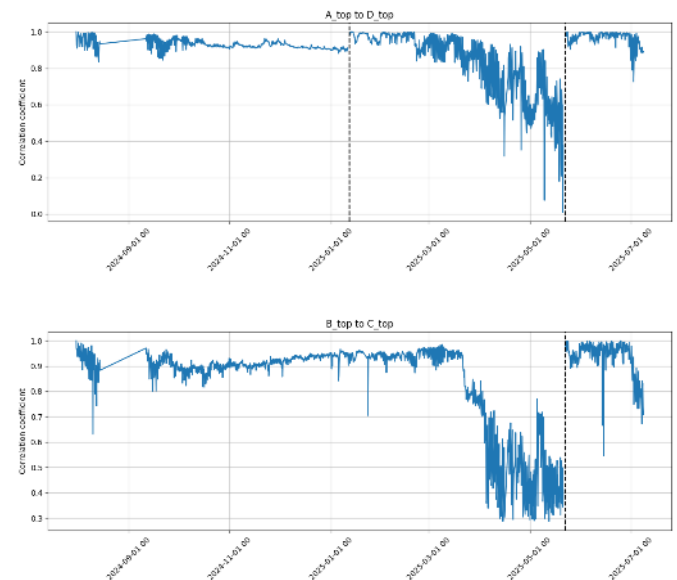


Figure 5-12 Correlation coefficient relative to previous event.

An example is shown in Figure 5-12. For 2024 the graphs are identical to method 1 as shown in Figure 5-10. For sensor pair A-D a sudden and significant change occurred in January 2025, which is marked with a vertical dashed line. Just after this

change a new reference measurement was selected, and the correlation coefficients after this time are calculated relative to this new reference. There's also a vertical dotted line in early May 2025. On this day the triggering system was reconfigured to improve time-accuracy. Therefore all measurements after this reconfiguration are compared to the first measurements since reconfiguration.

With this new processing it is clear that the low correlation coefficients of Figure 5-10 are not due to sensor degradation, since a new reference measurement can significantly improve the results. It is likely that the sudden drops in correlation coefficients are caused by structural changes in the bridge, and may be indicative of damage.

Further research is needed to determine the cause of some the low correlation outliers. A load tests with a known vehicle might be informative to relate the calculated stretch-coefficients to stress & strain. Further modelling of measured temperature gradients with a heat-flow model might also give a better understanding of the internal stress due to temperature gradients.

6 CONCLUSION

After well over a year of measurements, both types of temperature sensors remain operational. Suggesting there is no need for expensive analog temperature sensors and related cabling and AD converters. Cheap DS18B20 are accurate and reliable.

The Smart-Aggregate system has also performed well. While SA's are mainly used in short-term tests in the lab, our results show a life expectancy of at least 210 thousand pulses transmitted and/or received.

Work on the wear-layer of the deck is clearly visible in the correlation coefficient of sensors that are placed well below deck. Suggesting the sensors work well for long-term monitoring of structural changes. After the replacement of the wear-layer the daily variation in correlation coefficients has increased.

The selection of the reference measurement for stretching calculation has a significant influence on the resulting correlation coefficients and stretch factors. Using a fixed baseline is unfeasible because the correlation coefficient slowly degrades. Using a moving baseline however decreases insight in progressive changes. It is suggested to use a piecewise approach, where significant degradation of the correlation coefficient triggers a new reference measurement.

Results are strongly influenced by temperature, and this requires further study to separate the effects of temperature gradients from effects due to structural changes. It is advised to study this using a (simpler) statically determinate structure, where temperature gradients only result in strains, and not in stress. In this way the phenomena can be decoupled.

REFERENCES

- [1] H. Cheng, Y. Yang, F. Besseling, C. Kortendijk, A. Hoekstra, Monitoring the concrete slab bridge on Balladelaan in the Netherlands using embedded ultrasonic sensors, Proceeding of the IABSE Congress Gent, 2025
- [2] Cheng, H.; Weemstra, C.; Hendriks, M. A. N.; Yang, Y., Comparing the stretching technique and the wavelet cross-spectrum technique for measuring stress-induced wave-velocity changes in concrete. *Autom. Constr.* **2024**, 158, 105221.

- [3] Song G, Gu H, Mo YL (2008) Smart aggregates: multi-functional sensors for concrete structures-a tutorial and a review. *Smart Materials and Structures* 17(3). <https://doi.org/10.1088/0964-1726/17/3/033001>